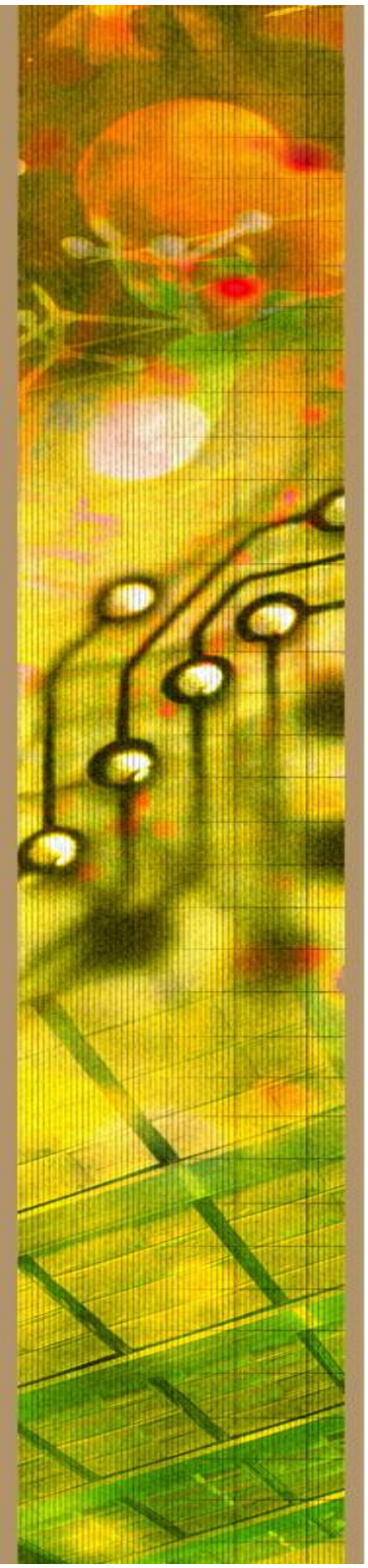

Modeling of melt layer erosion during plasma instabilities

Gennady V. Miloshevsky

Ahmed Hassanein

Purdue University, West Lafayette, Indiana

Presented at Plasma Facing Components Community Meeting MIT, Cambridge, USA, July 08-10, 2009

PURDUE NUCLEAR ENGINEERING

PURDUE UNIVERSITY

Outline

- **Background**
- **New Two-Fluid Computational Model**
- **Benchmark Problems**
- **Kelvin-Helmholtz Instability**
- **Simulation Results**
- **Conclusions & Future Work**

Background

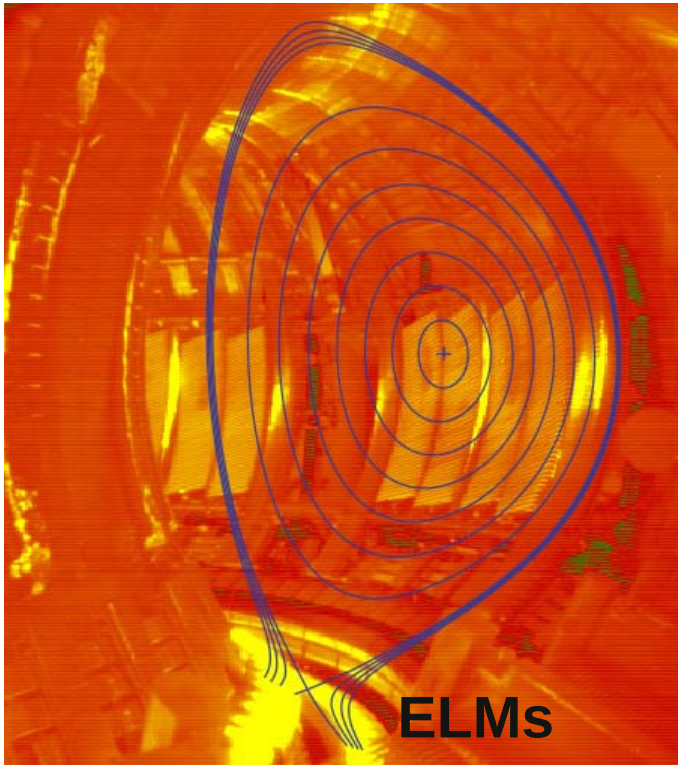

J.PAMELA, V. PHILIPPS 18 (36) 17th PSI Conference, Hefei, China 22 May 2006

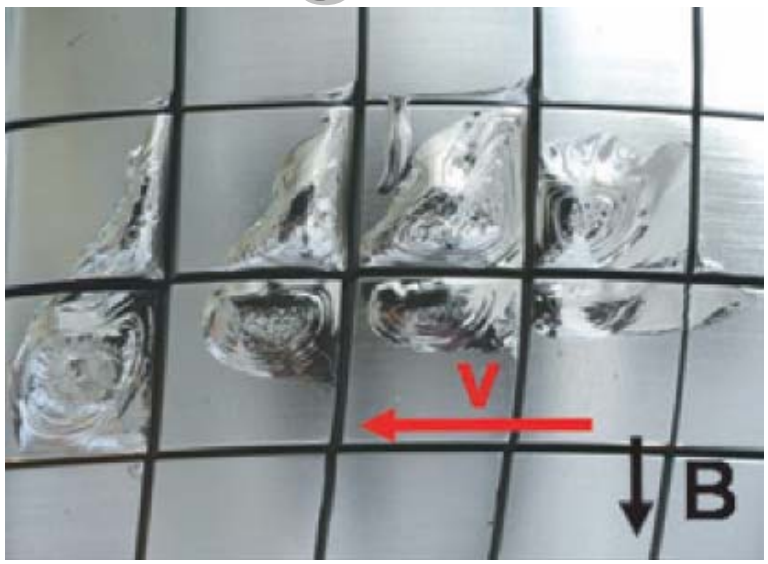

Tungsten plate in TEXTOR tokamak
Sergienko et al., Phys. Scr. T128 (2007) 81

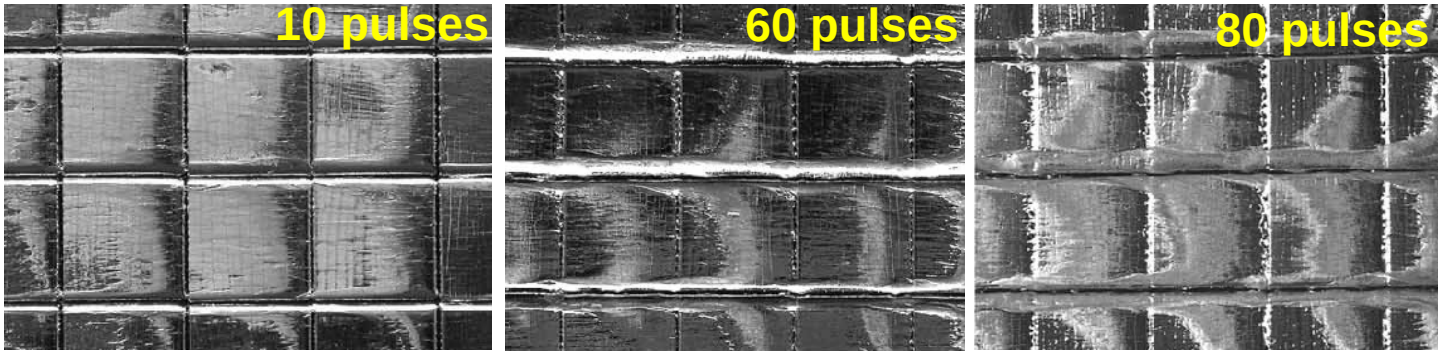

Tungsten plate in QSPA and MK-200UG plasma guns
Federici et al., Journal of Nuclear Materials 337–339 (2005) 684

- **High erosion due to the loss of tungsten melt layer**
- **Ablation physics of macroscopic material is the governing mechanism**
- **The melt loss is due to plasma impact and/or Lorentz force**

Background

~0.5–2.5 MJ/m^2
~0.4–0.6 ms

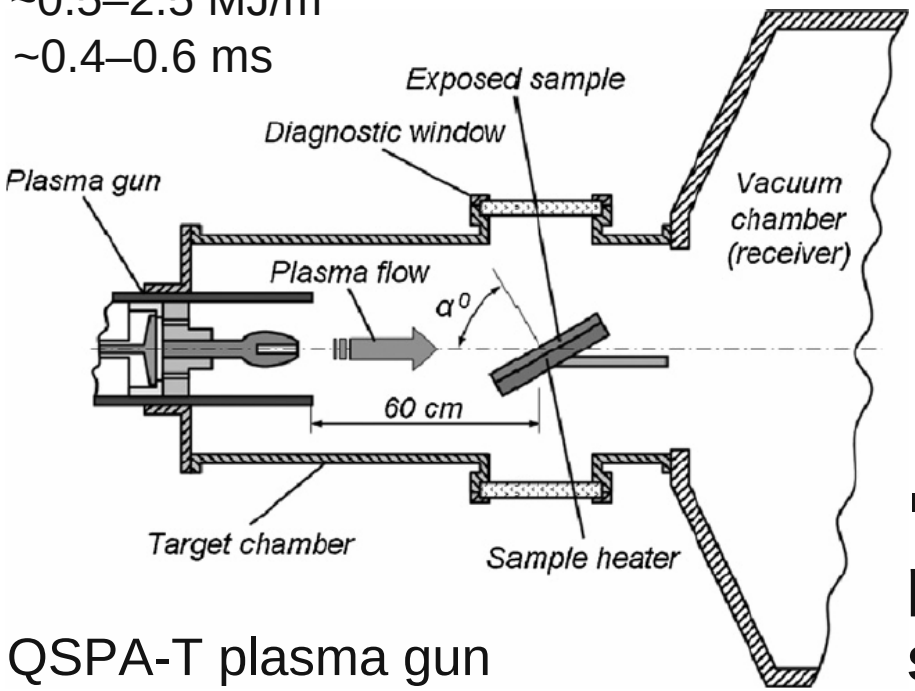

QSPA-T plasma gun
Bazylev et al., Fusion Engineering and Design 84 (2009) 441

- **melt layer erosion due to splashing of liquid tungsten droplets**
- **main physical mechanism – Kelvin-Helmholtz instability generated by a plasma flow**
- **NO REAL NUMERICAL SIMULATION phenomenological model: growth of surface waves, droplet formation and melt layer losses are estimated**

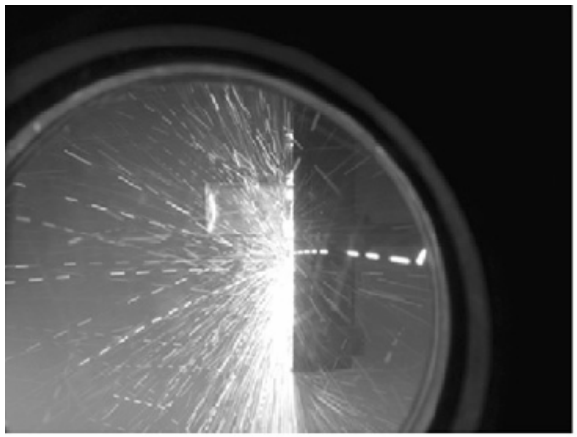
Q = 2.0 MJ/m^2 , p = 3.2 atm

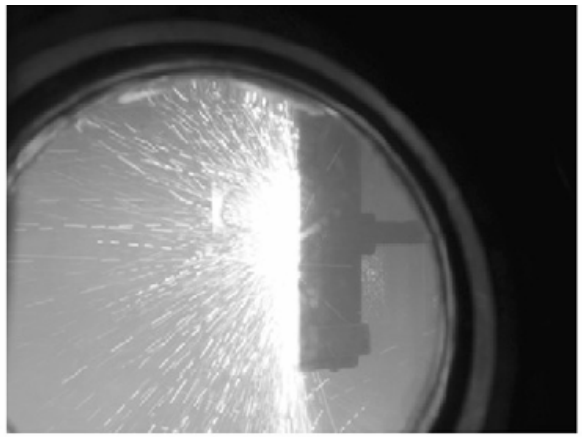
Q = 2.2 MJ/m^2, p = 4 atm

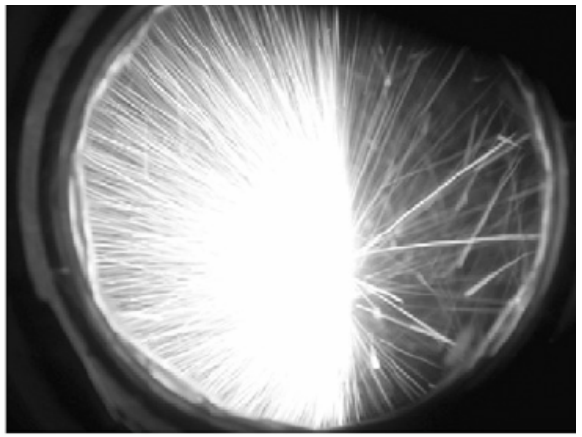
Q > 2.2 MJ/m^2 , p = 5 atm

Challenges of Computer Modelling

- different physical and thermodynamic properties of plasma-gas and liquid-tungsten fluids – two-fluid computational model is needed
- immiscible pure fluids (plasma and liquid) separated by sharp interface – its high resolution is needed
- large density ratios ~10^{8}-10^{10} between plasma (~10^{-8} g/cm^{3}) and liquid tungsten (~17.6 g/cm^{3}) – no understanding of K-H instability for this case
- essentially nonlinear aspects of K-H instability, complex nature of interfacial dynamics involving development, grows, breakup of vortices and formation of droplets – high resolution simulations are needed

Two-Fluid Computational Model

Mass conservation: ***gas and liquid phase***

$$\frac{\partial \alpha_g \rho_g}{\partial t} + \frac{\partial \alpha_g \rho_g u_g}{\partial x} + \frac{\partial \alpha_g \rho_g v_g}{\partial y} + \frac{\partial \alpha_g \rho_g w_g}{\partial z} = 0$$

$$\frac{\partial \alpha_l \rho_l}{\partial t} + \frac{\partial \alpha_l \rho_l u_l}{\partial x} + \frac{\partial \alpha_l \rho_l v_l}{\partial y} + \frac{\partial \alpha_l \rho_l w_l}{\partial z} = 0$$

α_g and α_l - gas and liquid volume fractions

$$\alpha_g + \alpha_l = 1$$

Two-Fluid Computational Model

Momentum conservation: ***gas phase***

$$\frac{\partial \alpha_g \rho_g u_g}{\partial t} + \frac{\partial}{\partial x}\left(\alpha_g \rho_g u_g^2 + \alpha_g p_g\right) + \frac{\partial}{\partial y}\left(\alpha_g \rho_g u_g v_g\right) + \frac{\partial}{\partial z}\left(\alpha_g \rho_g u_g w_g\right) =$$

$$= P_I \frac{\partial \alpha_g}{\partial x} + \lambda\left(u_l - u_g\right) - \alpha_g \rho_g g$$

$$\frac{\partial \alpha_g \rho_g v_g}{\partial t} + \frac{\partial}{\partial x}\left(\alpha_g \rho_g v_g u_g\right) + \frac{\partial}{\partial y}\left(\alpha_g \rho_g v_g^2 + \alpha_g p_g\right) + \frac{\partial}{\partial z}\left(\alpha_g \rho_g v_g w_g\right) =$$

$$= P_I \frac{\partial \alpha_g}{\partial y} + \lambda\left(v_l - v_g\right)$$

$$\frac{\partial \alpha_g \rho_g w_g}{\partial t} + \frac{\partial}{\partial x}\left(\alpha_g \rho_g w_g u_g\right) + \frac{\partial}{\partial y}\left(\alpha_g \rho_g w_g v_g\right) + \frac{\partial}{\partial y}\left(\alpha_g \rho_g w_g^2 + \alpha_g p_g\right) =$$

$$= P_I \frac{\partial \alpha_g}{\partial z} + \lambda\left(w_l - w_g\right)$$

Two-Fluid Computational Model

Momentum conservation: ***liquid phase***

$$\frac{\partial \alpha_l \rho_l u_l}{\partial t} + \frac{\partial}{\partial x}\left(\alpha_l \rho_l u_l^2 + \alpha_l p_l\right) + \frac{\partial}{\partial y}\left(\alpha_l \rho_l u_l v_l\right) + \frac{\partial}{\partial z}\left(\alpha_l \rho_l u_l w_l\right) =$$

$$= -P_I \frac{\partial \alpha_g}{\partial x} - \lambda(u_l - u_g) - \alpha_l \rho_l g$$

$$\frac{\partial \alpha_l \rho_l v_l}{\partial t} + \frac{\partial}{\partial x}\left(\alpha_l \rho_l v_l u_l\right) + \frac{\partial}{\partial y}\left(\alpha_l \rho_l v_l^2 + \alpha_l p_l\right) + \frac{\partial}{\partial z}\left(\alpha_l \rho_l v_l w_l\right) =$$

$$= -P_I \frac{\partial \alpha_g}{\partial y} - \lambda(v_l - v_g)$$

$$\frac{\partial \alpha_l \rho_l w_l}{\partial t} + \frac{\partial}{\partial x}\left(\alpha_l \rho_l w_l u_l\right) + \frac{\partial}{\partial y}\left(\alpha_l \rho_l w_l v_l\right) + \frac{\partial}{\partial y}\left(\alpha_l \rho_l w_l^2 + \alpha_l p_l\right) =$$

$$= -P_I \frac{\partial \alpha_g}{\partial z} - \lambda(w_l - w_g)$$

Two-Fluid Computational Model

Energy conservation: ***gas and liquid phase***

$$\frac{\partial \alpha_g E_g}{\partial t}+\frac{\partial}{\partial x}\left(u_g(\alpha_g E_g+\alpha_g p_g)\right)+\frac{\partial}{\partial y}\left(v_g(\alpha_g E_g+\alpha_g p_g)\right)+\frac{\partial}{\partial z}\left(w_g(\alpha_g E_g+\alpha_g p_g)\right)=$$

$$=U_I P_I\frac{\partial \alpha_g}{\partial x}+V_I P_I\frac{\partial \alpha_g}{\partial y}+W_I P_I\frac{\partial \alpha_g}{\partial z}+\mu P_I\left(p_l+\sigma\kappa-p_g\right)+$$

$$+\lambda U_I(u_l-u_g)+\lambda V_I(v_l-v_g)+\lambda W_I(w_l-w_g)-\alpha_g\rho_g u_g g$$

$$\frac{\partial \alpha_l E_l}{\partial t}+\frac{\partial}{\partial x}\left(u_l(\alpha_l E_l+\alpha_l p_l)\right)+\frac{\partial}{\partial y}\left(v_l(\alpha_l E_l+\alpha_l p_l)\right)+\frac{\partial}{\partial z}\left(w_l(\alpha_l E_l+\alpha_l p_l)\right)=$$

$$=-U_I P_I\frac{\partial \alpha_g}{\partial x}-V_I P_I\frac{\partial \alpha_g}{\partial y}-W_I P_I\frac{\partial \alpha_g}{\partial z}-\mu P_I\left(p_l+\sigma\kappa-p_g\right)-$$

$$-\lambda U_I(u_l-u_g)-\lambda V_I(v_l-v_g)-\lambda W_I(w_l-w_g)-\alpha_l\rho_l u_l g$$

σ – surface tension coefficient; for tungsten σ =2300 dyn/cm

$\kappa=-\nabla\cdot\left(\frac{\nabla\alpha_l}{|\nabla\alpha_l|}\right)$ - interface curvature

Two-Fluid Computational Model

Volume fraction equation

$$\frac{\partial \alpha_g}{\partial t} + U_I \frac{\partial \alpha_g}{\partial x} + V_I \frac{\partial \alpha_g}{\partial y} + W_I \frac{\partial \alpha_g}{\partial z} = -\mu\left(p_l + \sigma\kappa - p_g\right)$$

Stiffened equations of state

$$\rho_g e_g = (p_g + \gamma_g P_{\infty,g})/(\gamma_g - 1); \quad \rho_l e_l = (p_l + \gamma_l P_{\infty,l})/(\gamma_l - 1).$$

$$E_g = \frac{1}{2}\rho_g(u_g^2 + v_g^2 + w_g^2) + \rho_g e_g; \quad E_l = \frac{1}{2}\rho_l(u_l^2 + v_l^2 + w_l^2) + \rho_l e_l.$$

Interface pressure and velocities

$$P_I = \alpha_g p_g + \alpha_l p_l; \quad U_I = \frac{\alpha_g \rho_g u_g + \alpha_l \rho_l u_l}{\alpha_g \rho_g + \alpha_l \rho_l};$$

$$V_I = \frac{\alpha_g \rho_g v_g + \alpha_l \rho_l v_l}{\alpha_g \rho_g + \alpha_l \rho_l}; \quad W_I = \frac{\alpha_g \rho_g w_g + \alpha_l \rho_l w_l}{\alpha_g \rho_g + \alpha_l \rho_l}.$$

for tungsten:

$\gamma_l = 2.2$

$P_{\infty,l} = 1.41\ Mbar$

Two-Fluid Computational Model

- fluids with different physical and thermodynamic properties (out of thermodynamic equilibrium)
- fluids are separated by sharp interface and co-exist at every point in space and time with certain volume fractions

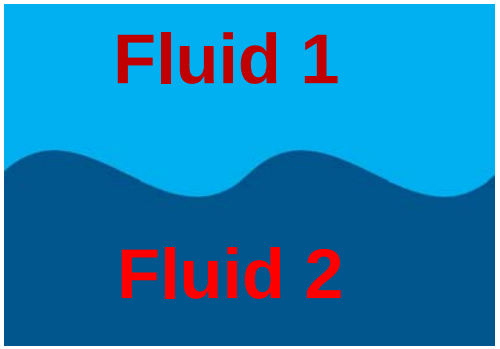

- each fluid is governed by its own set of balance equations closed by its own equation of state
- pressure and velocity relaxation procedures are used to establish the mechanical equilibrium between fluids
- source terms can be included for dissipative processes and phase transitions; equations for the number density of bubbles, granules, etc. can be added

Two-Fluid Computational Model

A two-step numerical approach is used to solve the system of eleven equations:

At step 1

- eleven two-phase flow equations are solved using the MUSCL-TVDLF hyperbolic solver
- second order MUSCL-TVDLF numerical scheme was elaborated, further developed and applied for the first time to the 3D system of two-fluid flows
- new feature – non-conservative volume fraction equation is solved simultaneously with the balance equations

At step 2

- instantaneous pressure and/(or if needed) velocity relaxation is performed to restore the equilibrium of the two fluids

Benchmark Problems

SIMPLE TESTS INVOLVING GAS-GAS FLUIDS : propagation of void waves; air-air and air-helium shock-tube tests; air-helium separation in a gravitational field

WATER-AIR SHOCK TUBE : a tube filled with water in the left hand side at high pressure and air in the right hand side with low pressure – to check method's ability to accurately capture strong contact waves

WATER FAUCET PROBLEM : water column flow in air annulus in a tube under the effect of gravity – to check method's ability to resolve volume fraction front

WATER-AIR SEPARATION PROBLEM : gravity-driven separation of water and air with transition from two-phase to one-phase state – to check method's ability to handle phase separation where one of the two fluids disappears locally

2D Air-Air Kelvin-Helmholtz Instability

roll up of initial horizontal air-air interface

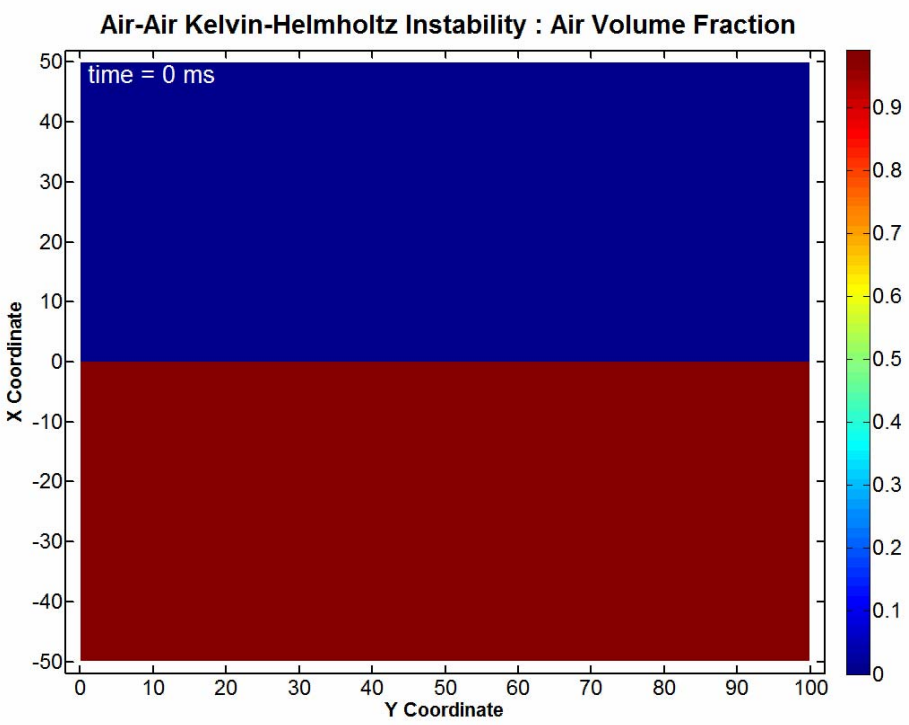

Speed 200 m/s

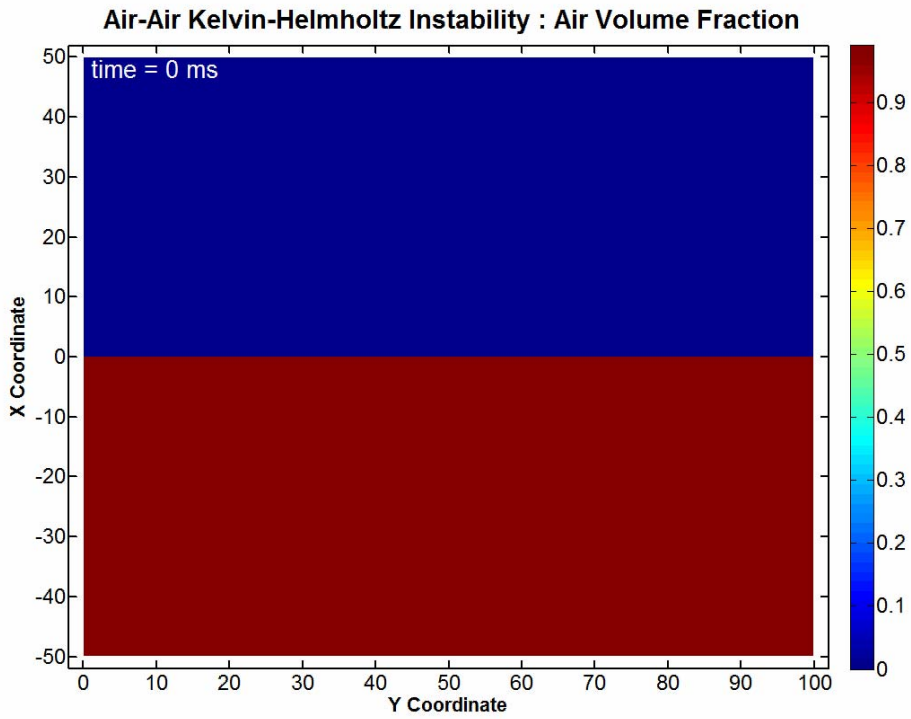

Speed 500 m/s

- development of saw-tooth-like secondary K-H instability (~4 ms for 200 m/s)
- formation of rib structures connecting the bottom of one roller to the top of the next (~8 ms for 200 m/s)
- collapse of rollers for supersonic relative speeds (500 m/s)

2D Air-Helium Kelvin-Helmholtz Instability

roll up of initial horizontal air-helium interface

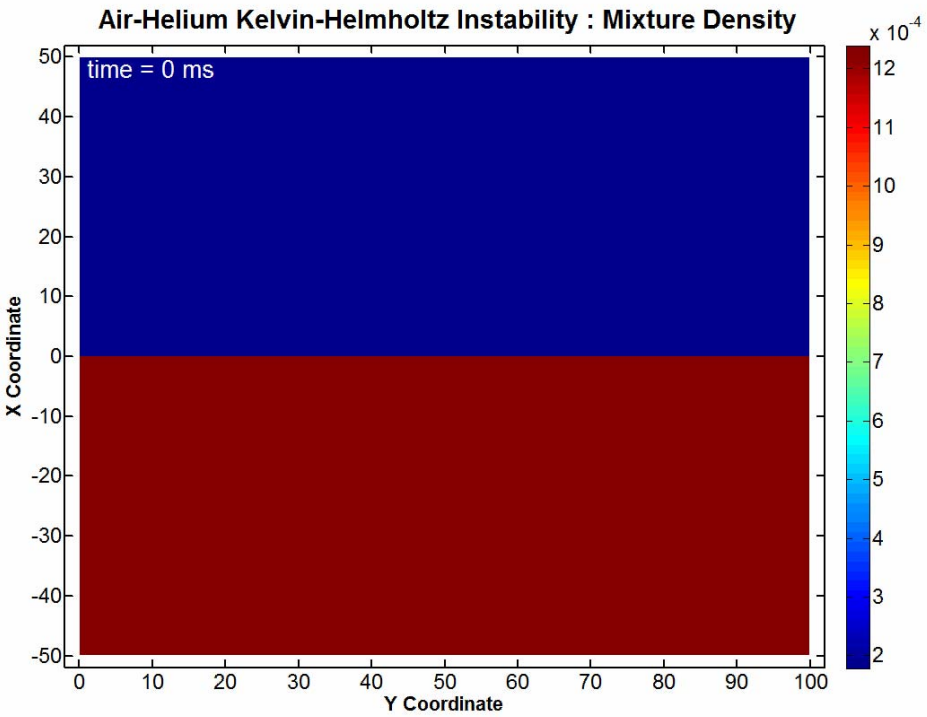

Speed 200 m/s

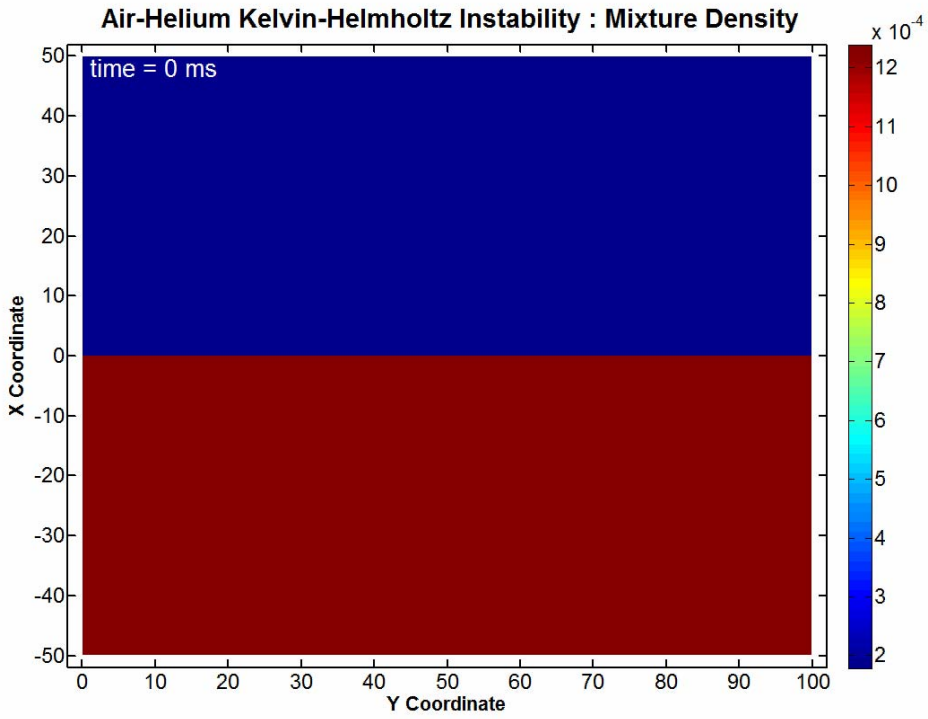

Speed 500 m/s

- broken vortex cores and development of spikes near the interface - variations in air density is necessary condition for K-H
- small vortices and broken droplets dominate in the late stages
- pinch-off of the interface with formation of droplets

Plasma-Liquid Tungsten Instability

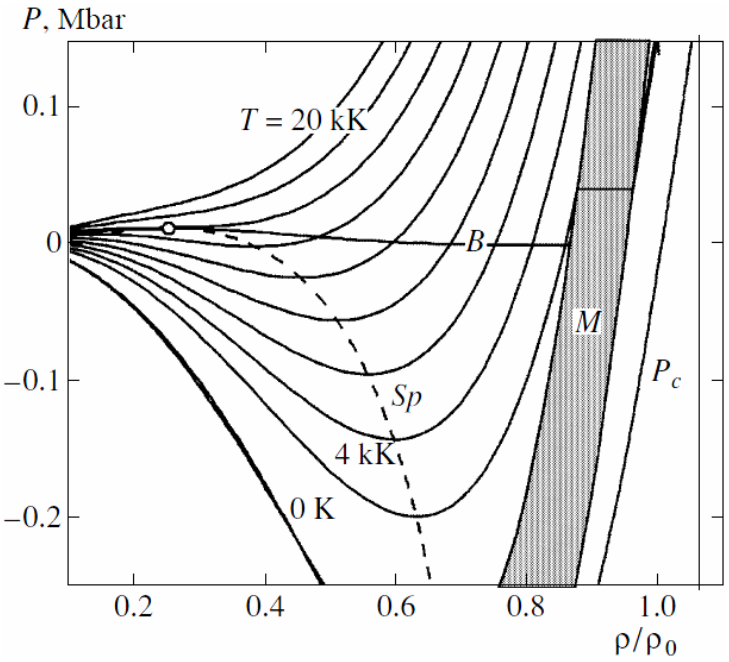

The state diagram of the fluid phase of tungsten. *Tkachenko et al., High Temperature, Vol. 39, 2001, pp. 674–687*

ρ_m~17.6 g/cm^3

ρ_m/ρ_0 ~ 0.91

T_m ~ 3695 K

P_m ~ 0.05 Mbar

c_m ~4.4 km/s

Initial set up:

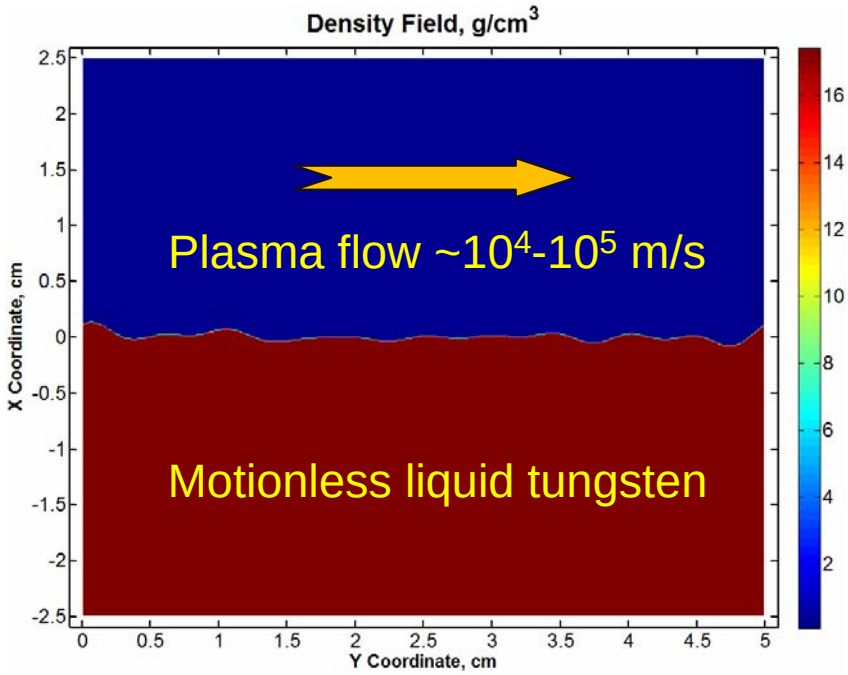

Stiff problem:

- slow liquid flow (very low Mach number) with weak density-pressure coupling
- liquid tungsten is essentially incompressible with insignificant variation in density even with a large plasma pressure gradient
- dense plasma with large pressure gradient is required to disturb the liquid density field and generate surface waves

Plasma-Liquid Tungsten Instability

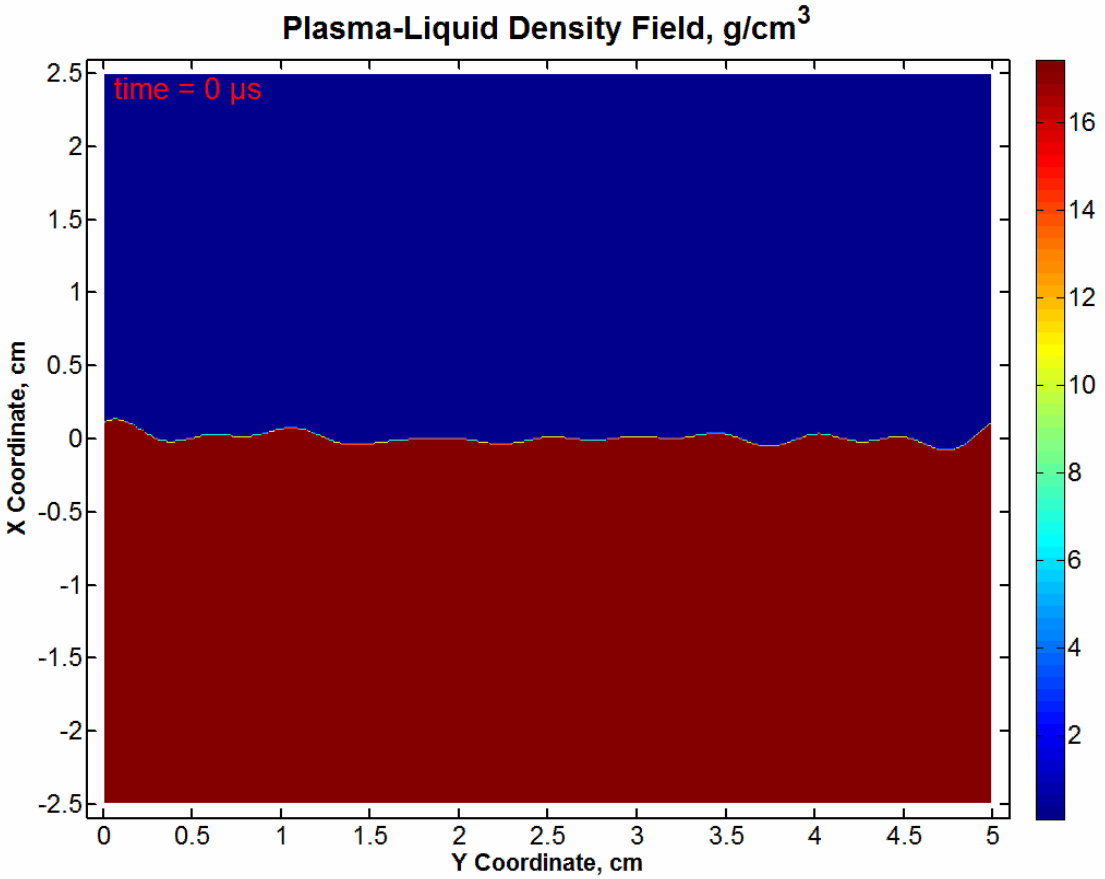

Plasma-liquid interface with random initial perturbation

Plasma density: ~0.01 g/cm^3

Plasma speed: ~10^4 m/s

- disruption of the interface within the melt depth ~1 cm
- formation of liquid plumes, fingers and droplets drugged by the plasma flow
- topological structure of liquid patters is highly irregular – no periodic array of compact spanwise K-H rollers
- velocity of liquid metal motion is ~2-5 m/s deeply inside the melt layer; the velocity of melt fragments reaches up to ~150 m/s at the surface

Plasma-Liquid Tungsten Instability

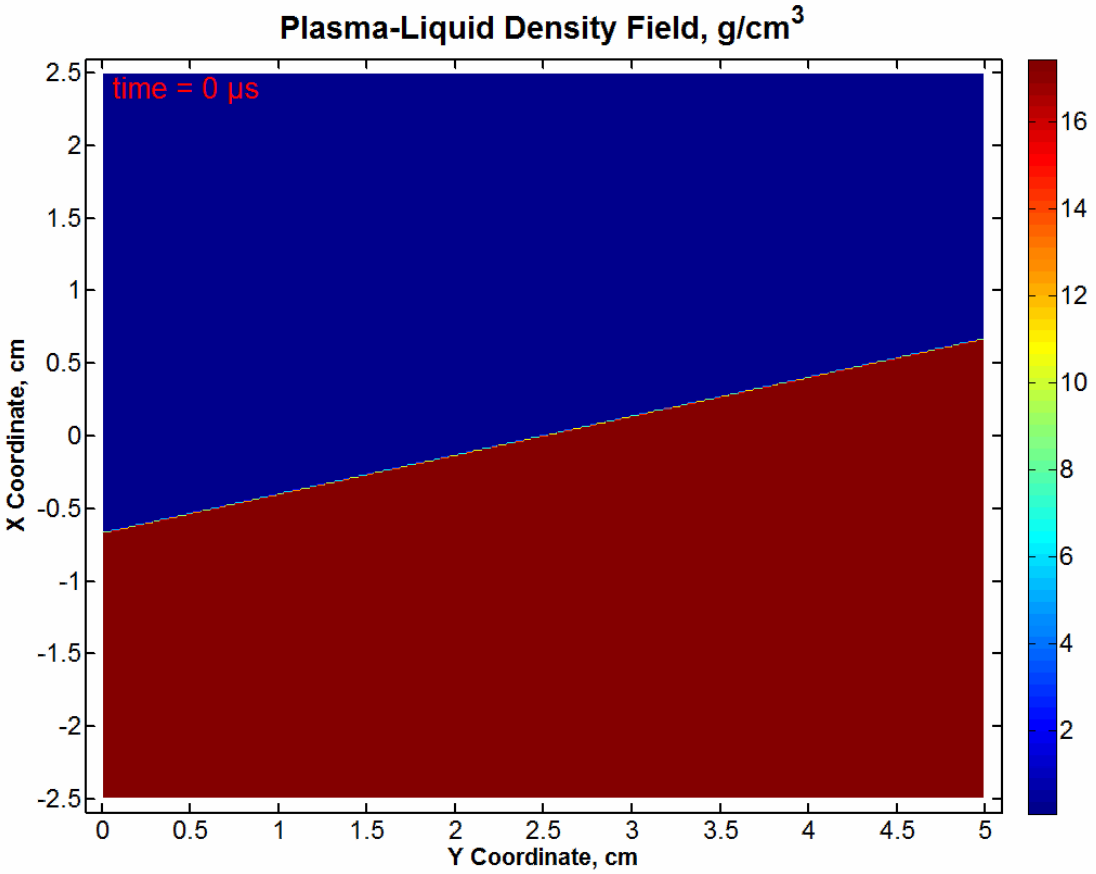

Impact of plasma jet on inclined (~15^0) melt layer

Plasma density: ~0.1 g/cm^3

Plasma speed: ~$5 \cdot 10^3$ m/s

- generation of waves starting at the impact place and propagating along the melt surface
- development of liquid plumes, fingers and droplets
- initial growth of spikes on the molten metal surface leads to fragmentation of the melt layer at later times
- the impulse of the plasma jet on the melt affects the bulk of the melt layer with formation of large particle fragments

Plasma-Liquid Tungsten Instability

1. ***Kelvin–Helmholtz instability mechanism:***

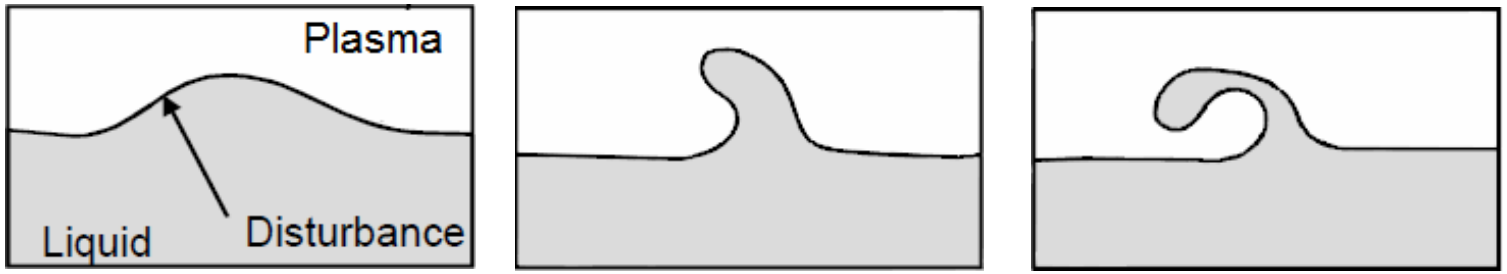

- surface waves amplify forming finger-like projections that break off to form droplets
- depth of the melt affected is of the order of the wavelength of the surface disturbance

2. ***Plasma-driven flow instability mechanism:***

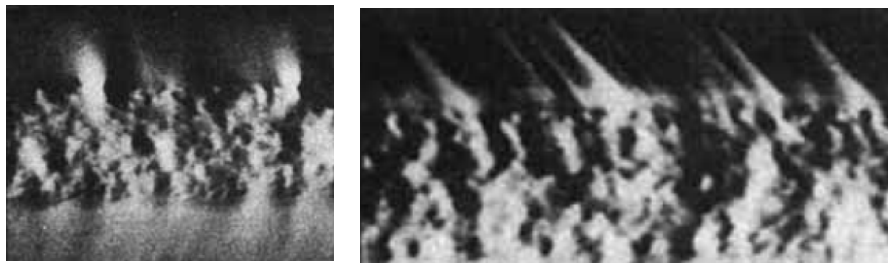

- large droplets can be blown out by shear forces acting on the bulk of the molten metal
- impulse of the plasma flow can cause bulk fragmentation of the melt layer with ejection of large particle fragments

Conclusions

- two-fluid numerical model is able to resolve topological structures of highly complicated flows that arise at the plasma-liquid interface of a melted tungsten layer
- REQUIRED condition for development of instability - variations and changes in the density field of liquid tungsten caused by the plasma flow – not observed for low-density plasma
- high-speed (~10^4-10^5 m/s) and dense (>0.01 g/cm^3) plasma flows over the liquid tungsten surface can generate the ejection of droplets from a homogeneous melt layer due to bulk shear forces
- preliminary introduction of bubbles and density inhomogeneities into a melted layer can significantly change its behavior and cause ejection of droplets for lower plasma densities and speeds
- however, for ITER ELMs these predictions mean no tungsten melt splashing and droplet ejection due to the K-H instability induced by plasma flow; JxB force could be the main mechanism

Future Work

- implementation of the magnetic field and the effect of JxB force on a tungsten melt layer

- implementation of a solid-liquid tungsten boundary and prediction of liquid metal losses

- implementation of vapor bubbles and inhomogeneous boiling effects on the density field of a tungsten melt layer

- extensive computational runs using TeraGrid resources to investigate the flow regimes for tungsten melt splashing and formation of liquid droplets

Reserved Slides

Benchmark Problems

Water-Air Shock Tube : a tube filled with water in the left hand side at high pressure and air in the right hand side with low pressure

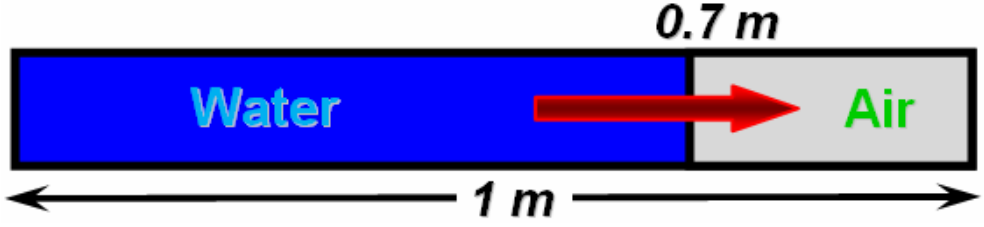

Initial data:

for $\leq 0.7\ m : \rho_l = 1000\ kg/m^3,\ P_l = 10^9\ Pa,\ u_l = 0\ m/s,\ \gamma_l = 4.4,\ \pi_l = 6 \cdot 10^8\ Pa,\ \alpha_l = 1 - \varepsilon;$

for $> 0.7\ m : \rho_g = 50\ kg/m^3,\ P_g = 10^5\ Pa,\ u_g = 0\ m/s,\ \gamma_g = 1.4,\ \pi_g = 0\ Pa,\ \alpha_g = 1 - \varepsilon;$

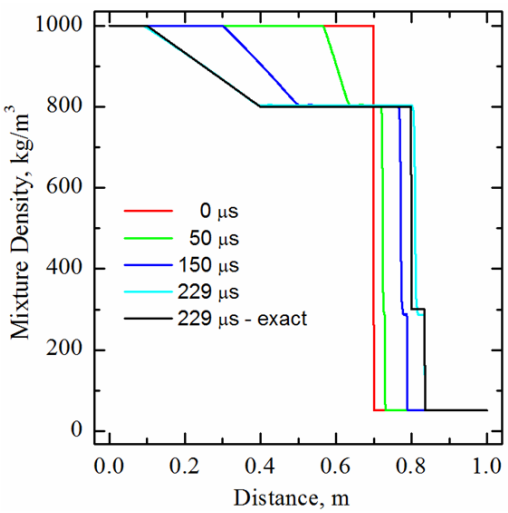

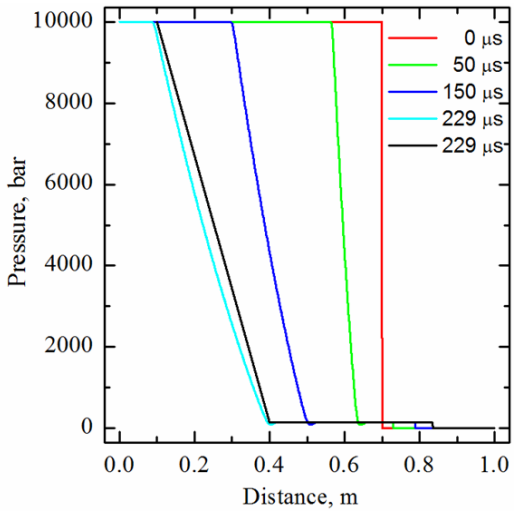

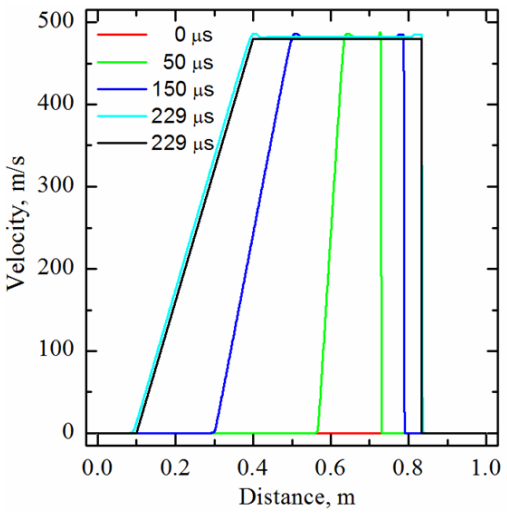

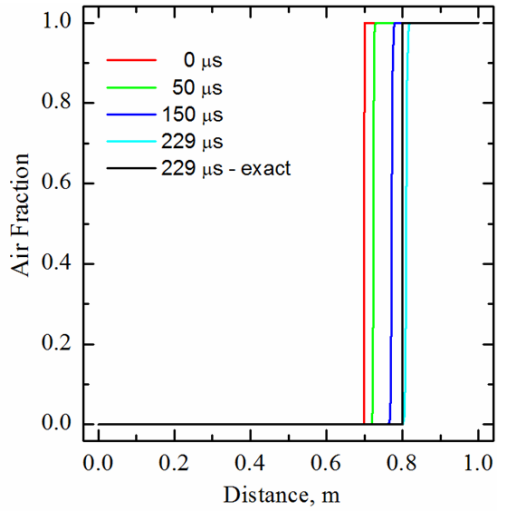

- instantaneous pressure and velocity relaxation procedures are used
- numerical method shows its ability to accurately capture strong contact waves
- agreement between the exact and numerical solutions is excellent, despite the stiffness of the problem (density ratio of 20 and pressure ratio of 10^4)

Benchmark Problems

WATER FAUCET PROBLEM: water column flow in air annulus in a tube under the effect of gravity

Initial data:

water: $\rho_l = 1000\ kg/m^3,\ P_l = 10^5\ Pa,\ u_l = 10\ m/s,\ \gamma_l = 4.4,\ \pi_l = 6 \cdot 10^8\ Pa,\ \alpha_l = 0.8;$

air: $\rho_g = 1\ kg/m^3,\ P_g = 10^5\ Pa,\ u_g = 0\ m/s,\ \gamma_g = 1.4,\ \pi_g = 0\ Pa,\ \alpha_g = 0.2;$

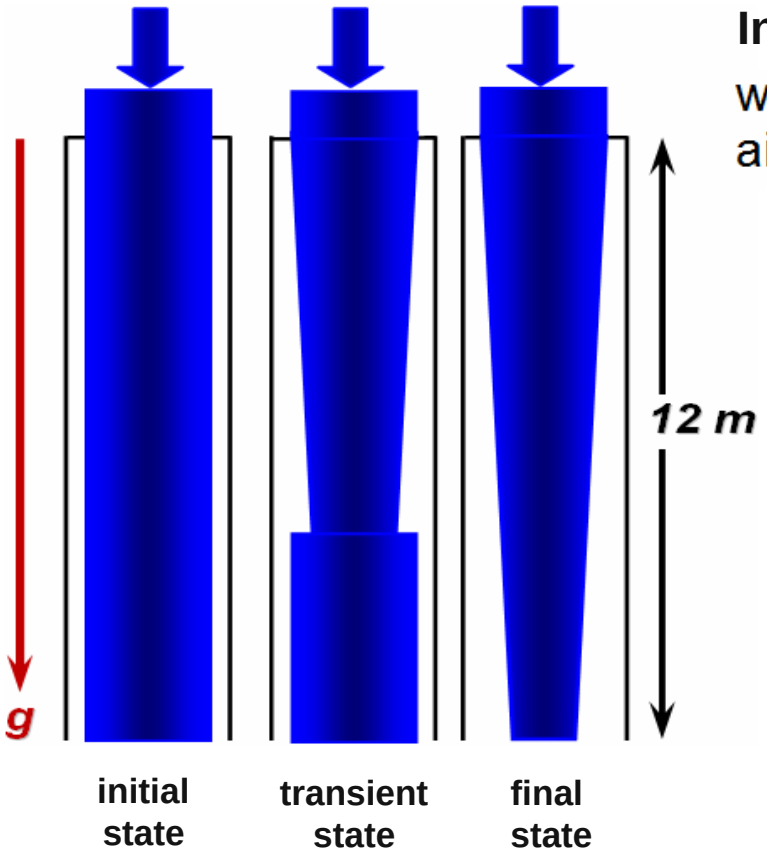

Inflow boundary conditions:

water: $u_l = 10\ m/s,\ \alpha_l = 0.8;$

air: $u_g = 0\ m/s,\ \alpha_g = 0.2;$

Outflow boundary conditions:

water: $P_l = 10^5\ Pa;$

air: $P_g = 10^5\ Pa;$

Approximate analytic solution:

$$u_l(x,t) = \begin{cases} \sqrt{2gx + (u_l^0)^2}, & for\ x \le u_l^0 t + 0.5gt^2, \\ u_l^0 + gt, & otherwise. \end{cases}$$

$$\alpha_g(x,t) = \begin{cases} 1 - \dfrac{\alpha_l^0 u_l^0}{\sqrt{2gx + (u_l^0)^2}}, & for\ x \le u_l^0 t + 0.5gt^2, \\ 0.2, & otherwise, \end{cases}$$

where $\alpha_l^0 = 0.8,\ u_l^0 = 10\ m/s$ and $g = 9.8\ m/s^2$

Benchmark Problems

WATER FAUCET PROBLEM: Numerical solution

- instantaneous pressure relaxation is used
- water and air possess their own velocities – no velocity relaxation is used

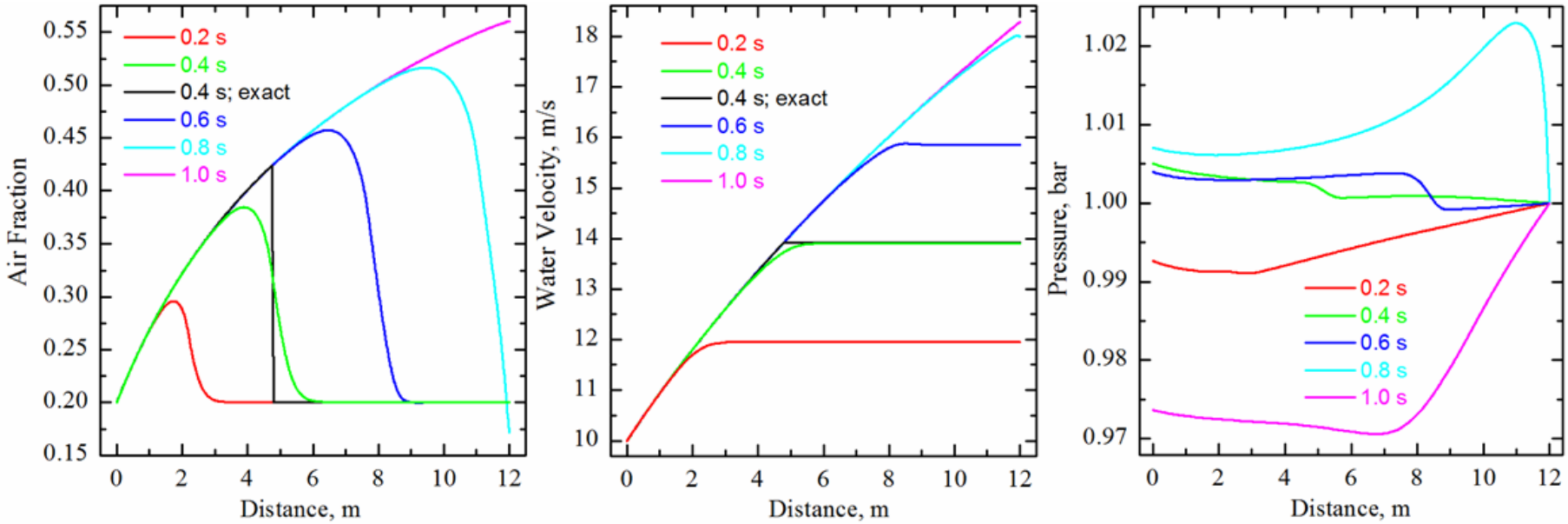

Transient air volume fraction, water velocity and pressure profiles at different times. Comparison between approximate analytic (black curves) and numerical air volume fraction and water velocity profiles at 0.4 s is shown. The numerical profiles are obtained using 5000 computational cells.

✓ numerical scheme is able to resolve volume fraction front

✓ pressure is not constant along the tube that leads to smearing of the air fraction interface; the approximate analytic solution was derived under the assumption of constant pressure

Benchmark Problems

Water-Air Separation Problem: gravity-driven separation of water and air

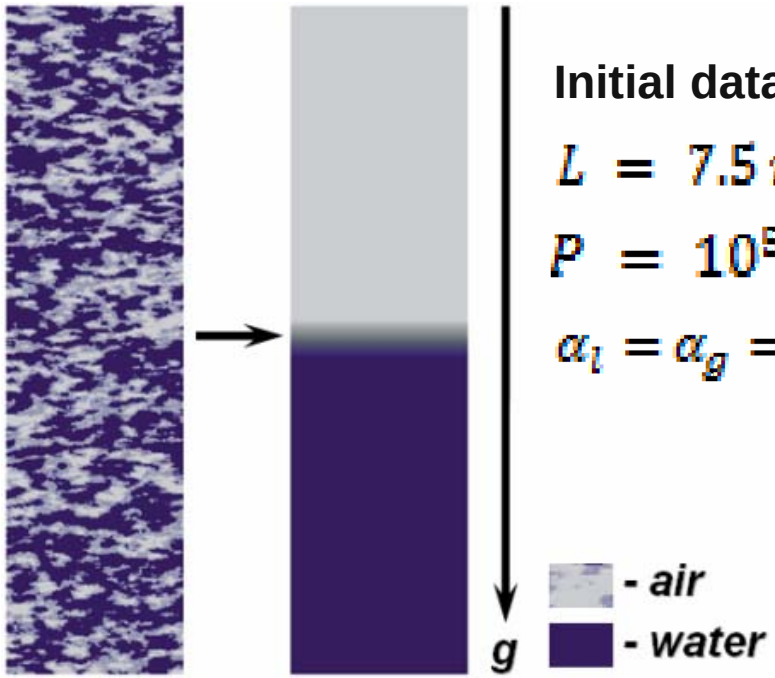

Approximate analytic solution:

$$\alpha_l(x,t) = \begin{cases} 0 & for\ x < 0.5gt^2, \\ 0.5 & for\ 0.5gt^2 \le x < L - 0.5gt^2, \\ 1 & for\ L - 0.5gt^2 < x, \end{cases}$$

$$u_l(x,t) = \begin{cases} \sqrt{2gx} & for\ x < 0.5gt^2, \\ gt & for\ 0.5gt^2 \le x < L - 0.5gt^2, \\ 0 & for\ L - 0.5gt^2 < x. \end{cases}$$

$t = \sqrt{L/g} \approx 0.87\ s$ - separation is finished

- transition from two-phase to one-phase state - a good test for the stability of the numerical scheme
- challenging problem for two reasons: 1) sharp variable gradients occur; 2) the volume fractions tend to approach 0 and 1

Benchmark Problems

Water-Air Separation Problem : Numerical solution

- instantaneous pressure relaxation is used; no velocity relaxation is used

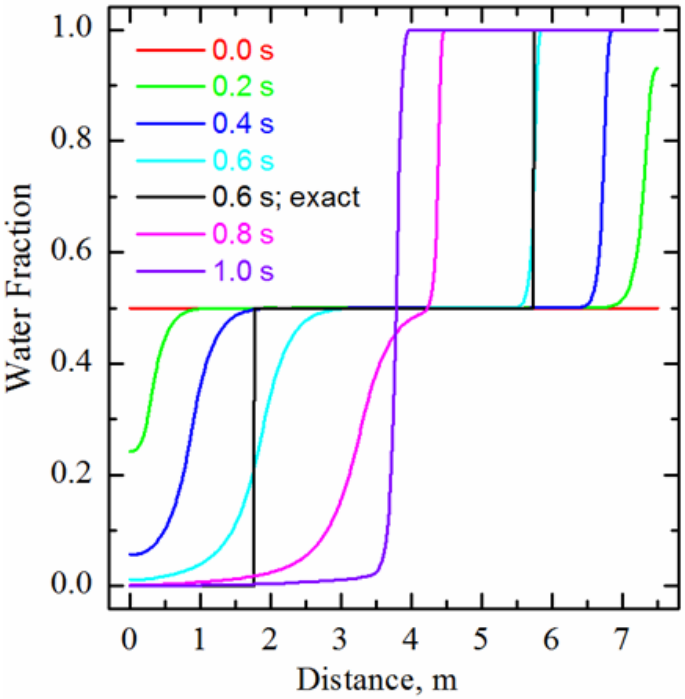

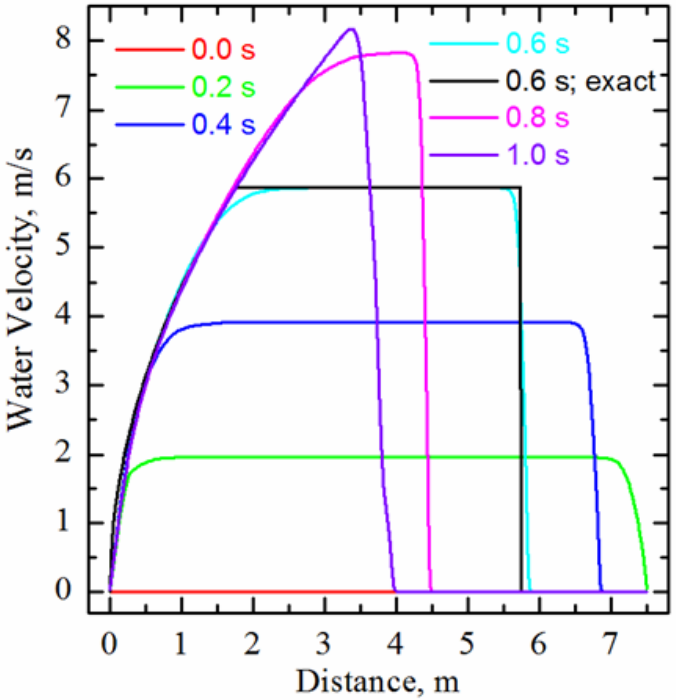

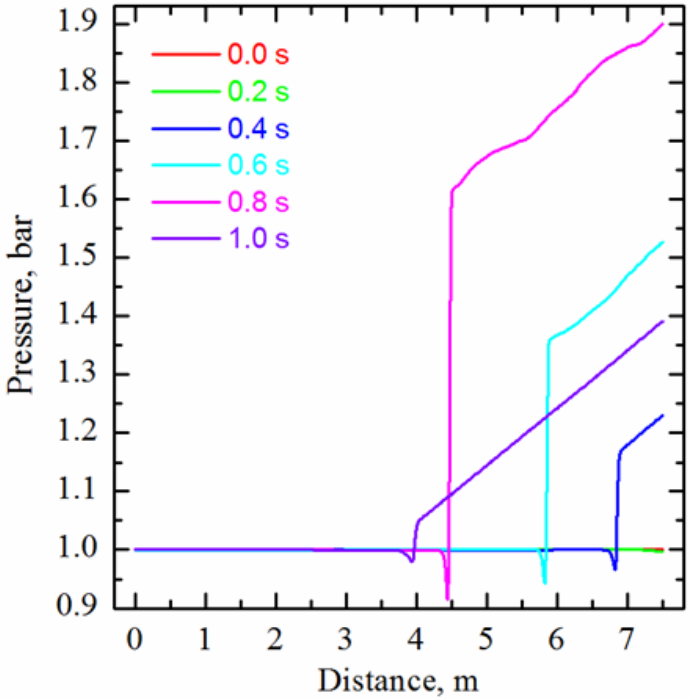

- numerical scheme can handle phase separation where one of the two fluids disappears locally (water at the top and air at the bottom of the tube)
- for the water volume fraction the resolution of the shock (to the right) is significantly sharper than that of the discontinuity (to the left); pressure increases about two time when the steady state is reached (~0.8 s) breaking the underlying assumption of constant pressure in analytic solution

Classical K-H Instability Analysis

Dispersion relation : perturbation ~ $\exp i(kx + \omega t)$

$$\omega = k\frac{\Delta U(\rho_2 - \rho_1)}{2(\rho_1 + \rho_2)} \pm \sqrt{\frac{\gamma k^3 + gk(\rho_2 - \rho_1)}{\rho_1 + \rho_2}\tanh(kh) - \frac{k^2(\Delta U)^2\rho_1\rho_2}{(\rho_1 + \rho_2)^2}}$$

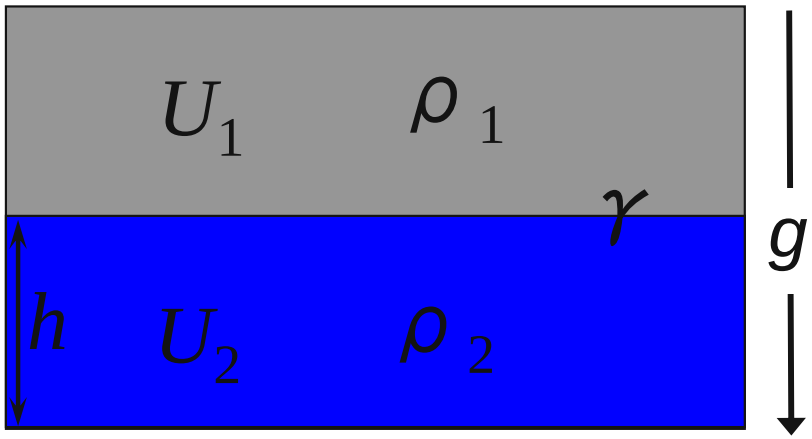

unstable if

$$(\Delta U)^2 > \frac{\rho_1 + \rho_2}{\rho_1\rho_2}\left(\gamma k + \frac{g}{k}(\rho_1 + \rho_2)\right)\tanh(kh)$$

with critical wavelength

$$\lambda_c = \frac{2\pi}{k_c} = 2\pi\left(\frac{\gamma}{g\,(\rho_2 - \rho_1)}\right)^{1/2}$$

For plasma-liquid tungsten:

$\gamma = 2300\ dyn/cm$ $\quad U_2 = 0\ cm/s$

$g = 981\ cm/s^2$ $\quad \rho_2 = 17.6\ g/cm^3$

$$U_1 = 10^5 \div 10^7\ cm/s$$

$$\rho_1 = 10^{-10} - 10^{-8}\ g/cm^3$$

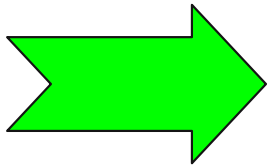

$\lambda_c \approx 3.6\ cm$

$U_1 > 10^6\ cm/s$